Simultaneous amplitude and frequency noise analysis in Chua's circuit.

J.-M. Friedt, D. Gillet, M. Planat
LPMO/CNRS, 32, avenue de l'observatoire, 25044 Besançon Cedex
`friedt@lpmo.univ-fcomte.fr`

Abstract

Chua's circuit is a non-linear electronic circuit stripped to its basic elements: a parallel LC circuit connected though a resistor to a parallel CN circuit, N being a non-linear conductance. Chua's circuit displays a complex evolution: period doubling pattern from a periodic oscillation to a chaotic behavior as one of the parameters of the circuit increases. We have decided to study statistical properties of the "instantaneous" frequency and amplitude signals when the inductor parameter L evolves.

We performed a large number of simultaneous frequency and amplitude data acquisitions which were validated by plotting the bifurcation diagrams as well as the standard and the Allan deviation.

1 Introduction

We studied the simultaneous evolution of the frequency and amplitude noise characteristics in a chaotic electronic circuit. The advantage of studying an electronic circuit, in addition to the fact that such circuits can be used for data transmission, is that a large number of samples can easily be obtained and thus statistically significant values can be computed. Chua's circuit strips a chaotic electronic circuit to its basic elements, and isolates the bifurcation parameter to a single component. We will here briefly describe the electronic circuit and the three coupled differential equations describing its behavior, the experimental setup we have developed in order to obtain experimental data, the method used for validating the data we recorded and finally the signal processing techniques we applied to these data.

1.1 Description of Chua's circuit

Chua's circuit is composed of two parallel circuits LC_1 and C_2N (N being a negative conductance characterized by two slopes, cf figure 1) connected by a resistor R (figure 1).

Chua's circuit is thus described by three coupled differential equations as follows. They are obtained by describing the intensity at nodes X and Y in figure 1 and the voltage at node X:

$$\begin{cases} C_1 \frac{dv_{C_1}}{dt} = \frac{1}{R}(v_{C_2} - v_{C_1}) - g(v_{C_1}) \\ C_2 \frac{dv_{C_2}}{dt} = \frac{1}{R}(v_{C_1} - v_{C_2}) + i_L \\ L \frac{di_L}{dt} = -v_{C_2} - i_L R_L \end{cases}$$

where R_L is the internal resistance of the inductor. In our circuit $R_L \simeq 3.3\ \Omega$, $C_1 \simeq 20.3$ nF, $C_2 \simeq 1847$ nF and $R \simeq 1.46$ kΩ.

As opposed to the equations leading to Rössler or Lorentz attractors [4, pp. 77 and 131] in which the nonlinearity is included as an explicit product between two of the differential equations variables, the only non linearity in this system comes from the equation including $g(v_{C_1})$ which describes the current to voltage response of the non-linear conductance N. A simulation of the current to voltage relation $I_N = g(V_N)$ is given in figure 1 (bottom) [5]:

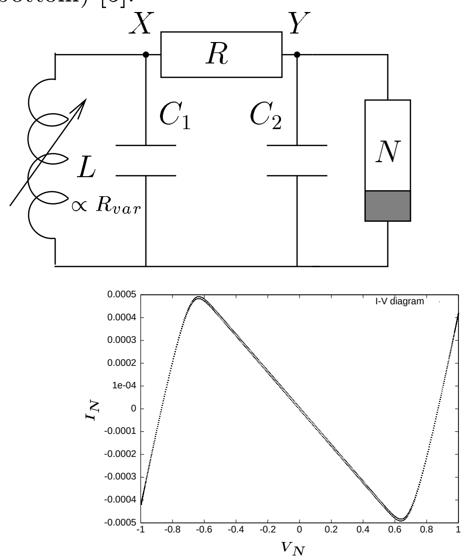

Fig 1: Schematic of Chua's circuit (top) and Spice simulation of the current to voltage characteristic of the non-linear element N (bottom).

We used a simulated inductor described by Weldon [1]: it is less voluminous and its value is defined by a variable resistor and thus can be computer controlled[1]

1.2 Data acquisition circuit

The three variables in Chua's circuit are the voltages at the two capacitors and the current running through the inductor. We have chosen for convenience to measure the voltage of one of the capacitors.

[1]The inductor's value L is related to that of the variable resistor R_{var}, which is the parameter shown in the figures of this article, from the relation $L = R_L \times (R_{var} + 30000) \times 0.1 \times 10^{-6}$ (30000 is the value of a resistor and 0.1×10^{-6} that of a capacitor).[1] With $0 < R_{var} < 24$ kΩ this leads to $L \sim 13.5$ mH ($\pm$ 4 mH).

The parameter we have chosen to vary is the inductor's value L. Our circuit includes an operational-amplifier based simulated inductor whose value is defined by a computer controlled variable resistor. This parameter is thus much simpler to modify than the capacitors' values. The circuit also evolves more smoothly by shifting the L value rather than the R value. The behavior of the oscillating circuit does not seem to have been perturbed when replacing the mechanical variable resistors with electronic, computer controlled variable resistors (they are usually used for remote controlled audio systems). We have been careful in separating the various power supplies (for Chua's circuit, analog signal pre-processing card, computer and data acquisition cards) and to insert buffers where the probes were reading the voltages.

We first attempted to estimate the oscillation frequency of Chua's circuit in its first periodic mode by replacing the non linear element N by a linear negative resistor of value R_N ($R_N \simeq -1300\ \Omega$). By additionally assuming that the internal resistance of the inductor is null ($R_L = 0$) we obtain a variable frequency $f = \frac{1}{2\pi}\sqrt{\frac{\frac{C_1}{L} - \frac{1}{R_N^2}}{C_1(C_1+C_2)}}$, versus L (figure 5, bottom). Numerical application with the values given previously, and for a value of the parameter $L = 14$ mH, gives $f \simeq 760$ Hz, in close agreement with the observed values. Adding the term that was at first neglected makes the literal solution much more complex (after solving using the software Maple V) and does not change the numerical estimation of the frequency.

The electronic circuit used for shaping the analog signals includes a follower circuit, followed by a comparator (for frequency measurements) and a peak holder (for amplitude measurements) made of a germanium diode (so as to minimize the voltage loss), a high value capacitor and an analog switch (so as to be able to discharge the capacitor and the reset the amplitude measurement).

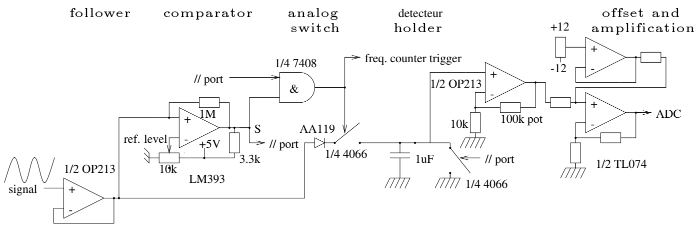

Fig 2: Schematic of the circuit used for measuring instantaneous frequency and the amplitude of the same period.

```
while S is high, wait
                              wait the end of the current period
set the ''AND'' gate triggering the frequency counter
                                    get ready for a measurement
while S is low, wait
                                        end of the low half-period
while S is high, wait
        end of the high half-period, measurement in progress
read amplitude and frequency measurements
                                                  data acquisition
capacitor reset
```

Measurement algorithm (this loop is executed for each new period to be measured)

We now understand that an acquisition only occurs when both the level of the voltage from Chua's circuit is higher than a given preset level (output S of the comparator) and the computer is ready for a new acquisition (second input of the "AND" gate set by the parallel port).

We have been able to verify, using a digital storagescope, that we indeed observed the expected signal: both amplitude (fig 3, top) and frequency (fig 3, middle) are measured on a single period. Amplitude must be read quickly, before the frequency, in order to avoid noise due to leakage currents coming from the analog switch (fig 3, bottom).

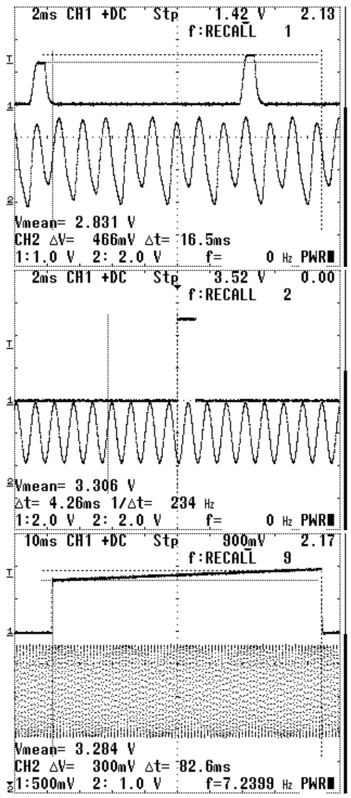

Fig 3: Storagescope outputs resulting from our data acquisition algorithm: top, the height of a pulse chosen randomly among the quasi-periodic signal is indeed proportional to the amplitude of this same period. Middle: the trigger pulse of the frequency

counter is indeed defined by the voltage going above a given preset value. Finally, bottom figure, the slow shift of the amplitude at the input of the analog to digital converter due to the leakage current leaving the analog switch. The conversion time during an actual acquisition is 70 times shorter than this pulse.

We found interesting that an experimental error lead to an optimized sweep of the value of the parameter L. As the computer controlled variable resistors we selected only allowed a choice of 64 resistance values, we decided to connect in series two variable resistors of different maximum values (10 and 50 kΩ) connected in parallel with fixed resistors so that the range of one of the variable resistors (10 kΩ) matches one step of the other variable resistor (50 kΩ). However, the composition law of resistors connected in parallel removes the linearity of adding the values of the two variable resistors connected in series. Hence, the composition of the successive values of the two variable resistors does not increase the resolution of each steps as expected, but gives a better distribution of the values taken by L than would have been obtained by connecting the two variable resistors in series, as shown figure 4.

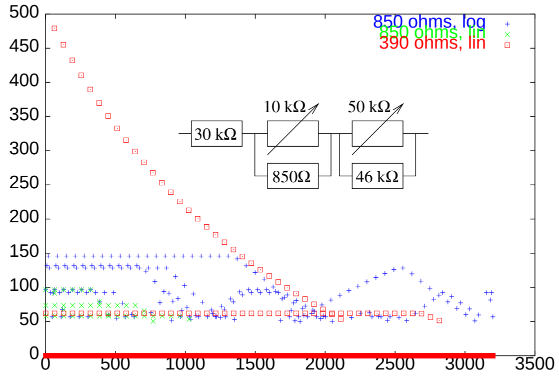

Fig 4: Difference between two successive values of the parameter L (as the sum of the resistance of the two variable resistors, each of which is in parallel with a constant resistor): comparison between various sweeping modes. The 50 kΩ variable resistor always sweeps a range from 0 to 39 kΩ in 50 linearly spaced steps (each of 780 Ω), while the 10 kΩ variable resistor sweeps either logarithmically (increases by 1, 2, 4, 8, 16 and 32 steps, resulting in $50 \times 7 = 350$ files) or linearly (10 kΩ increase in 64 steps, resulting in $50 \times 64 = 3200$ files). The curves shown on this figure result from varying the 10 kΩ variable resistor (lin or log) and the value of the resistance connected in parallel with this variable resistor (390 Ω – designed to fill the range between two steps of the 50 kΩ variable resistor – or 850 Ω – for which two successive ranges overlap and hence requiring some processing in order to put the files in the increasing values of R_{var}. We plotted here the resistance difference of R_{var} between two steps of the 10 kΩ variable resistor versus the index of the step.

2 Results

We graphically validated the data acquisition method (figure 5) by plotting the values taken by the amplitude and frequency time series versus the value of the L parameter. One can observe the first bifurcation, followed by the chaotic behavior. The widening of the frequency curve to the right of the graph (for large values of L) characterizes the transition from a Rössler-like attractor to a double scroll attractor, for which our measurements are harder to interpret (the separation of each period by the voltage crossing a reference level is no longer possible in this kind of oscillation mode as it was in the periodic regime).

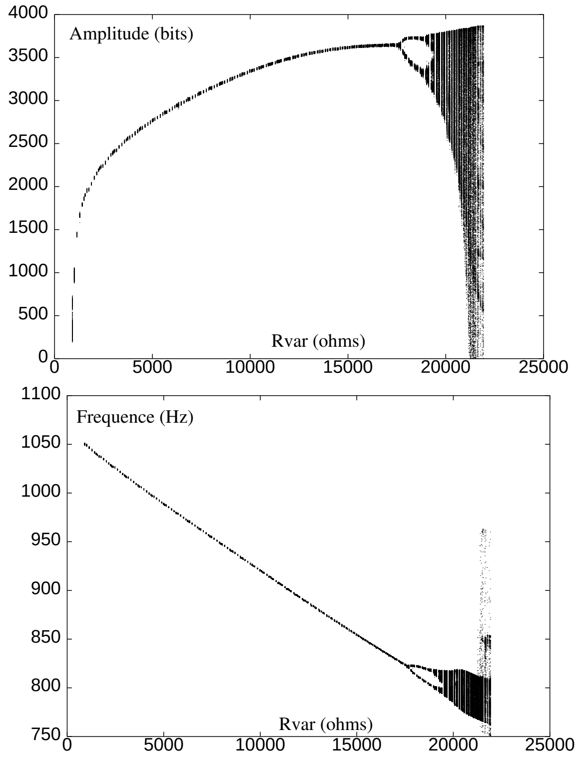

Fig 5: Bifurcation diagrams both in amplitude (top) and frequency (bottom). Each time series (plotted for a given abscissa corresponding to a value of the L parameter) includes 1000 points

2.1 Statistical results

As could be expected, the standard deviation quickly increases after the first bifurcation. This quick increase is partly due to our data analysis method as we do not separate various branches of the values taken by the time series (either in frequency or in amplitude) as such a distinction is no longer possible once the chaotic region is reached.

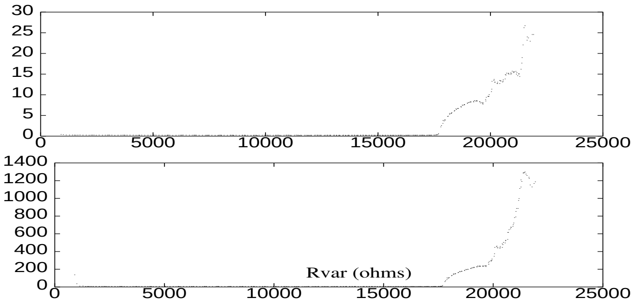

Fig 6: Evolution of the standard deviation with increasing values of the L parameter. Top: standard deviation of the frequency. Bottom: standard deviation of the amplitude.

An automatic measurement of the slope of Allan variance [3], although quite inaccurate, always gives an average value of -0.5, whatever the oscillation mode. This result means that the frequency noise is a white noise. However, this result must be interpreted as showing that our data acquisition algorithm randomly chooses a period in the oscillating signal – depending on the communication time of the GPIB interface between the frequency counter and the computer – rather than the statistics of the signal itself. We will see later that different results are obtained when studying continuous time series (including *all* periods in a given time interval) rather than values chosen randomly in the oscillating signals (figure 8).

2.2 Sequential results

While processing the data obtained statistically, we have developed a frequency-counter able to measure frequencies around 1 kHz with a 15 mHz resolution, and most importantly to send the result to the computer in less than half a millisecond (duration of half a period), allowing the measurement of the properties of all the consecutive periods in a given time lapse.

Obtaining data on all the periods in a given time lapse shows clearly the acquisition noise due to a coupling of Chua's oscillator with the 50 Hz signal from the electric mains. Bifurcation diagrams obtained with this new data acquisition mode are noisier than those obtained previously.

Obtaining all the periods in a given time lapse was confirmed by drawing the return maps for various oscillation regimes (figure 7).

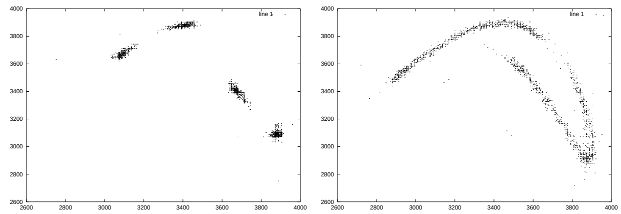

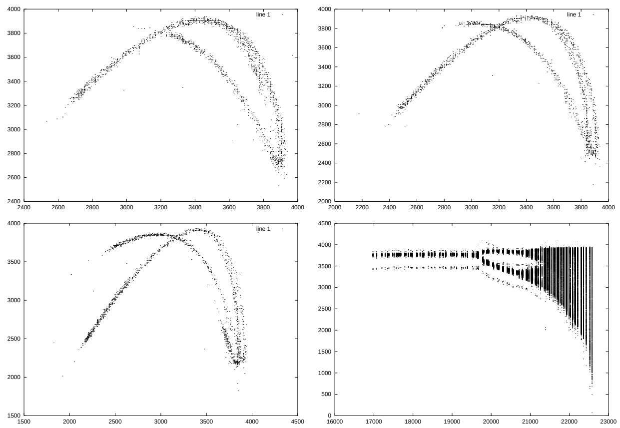

Fig 7: Return maps drawn for various oscillation regimes (from left to right and top to bottom, the R_{var} parameter is equal to 21254 Ω, 21484 Ω, 21711 Ω, 21933 Ω and 22151 Ω (which correspond respectively to values of 16.91 mH, 16.99 mH, 17.06 mH, 17.14 mH and 17.21 mH of L), and zoom on the bifurcation diagram's zone for which these return maps were shown

Allan variance is usually defined on frequency data. As we were not able to measure this variable quickly enough at the moment, we supposed as a first approximation that the behavior of the amplitude is similar to that of the frequency (as graphically shown by the bifurcation diagrams of fig. 5, although this hypothesis is still to be demonstrated). A first estimate of the slope of Allan variance versus the bifurcation parameter was thus computed on the sequential amplitude data (figure 8). We here expect, without being able to check this hypothesis, that the behavior of the amplitude noise is similar to that of the frequency noise.

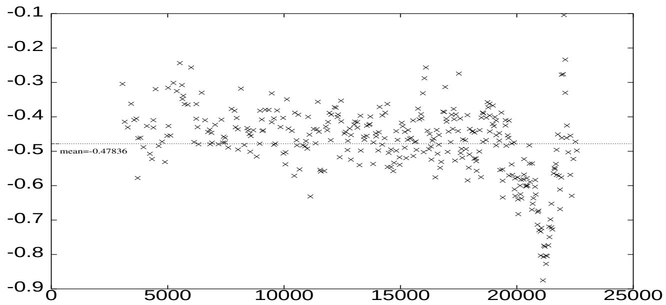

Fig 8: Evolution of the slope of Allan variance (computed on the experimental amplitude data) during the evolution from a periodic oscillation to a chaotic regime.

We observe a continuous evolution of Allan variance from a mean value of -0.5 (white frequency noise of thermal origin) to a slope of -1 when the circuit is in a chaotic regime. A slope of -1 of the Allan variance characterizes a noise spectrum of slope +1 or +2 (we have not yet been able to distinguish between the two regimes), originating respectively from electronic noise in the oscillator or an external white noise [3].

3 Conclusion

We have successfully built a circuit for statistically measuring instantaneous frequency and amplitude of Chua's circuit. We checked the validity of our results by plotting the bifurcation diagrams, and analyzed the standard deviation of the time series.

We then modified the acquisition algorithm in order to measure all instantaneous amplitudes in a given time lapse. Such measurements enable the evaluation of Allan variance. We showed that its slope evolves from -0.5 to -1 during the evolution of the behavior from periodic to chaotic. We furthermore displayed the return maps of the amplitude for various values of the bifurcation parameter.

Our future work includes completing a fast frequency counter. It will be combined with the fast frequency acquisition algorithm for simultaneous amplitude and frequency measurements of all periods in a given time lapse.

Another future research idea is to study the ability of neural networks, or simpler derivated algorithms, to effectively predict the evolution of the measured parameters (frequency and amplitude) of the chaotic circuit.

References

[1] Thomas P. Weldon, *An inductorless double scroll chaotic circuit*, Am. J. Phys **58** (10), October 1990

[2] R.N. Madan, *Chua's circuit: a paradigm for chaos*, World Scientific Series in Non-linear Science (Series B, vol 1) (1993)

[3] François Vernotte, *Approche multivariance du bruit de fréquence des oscillateurs*, Ann. Télécommun. **51** (9-10) (1996)

[4] P. Bergé, Y. Pomeau, Ch. Vidal, *L'ordre dans le chaos*, Hermann (1984)

[5] A. Tamaševičius, G. Mykolaitis, A. Namajunas, *Double scroll in a simple '2D' chaotic oscillator*, Electronics Letters **32** (14), July 4th 1996